

Use of an analytical model to determine the primary production from satellite data in a coastal upwelling environment

Satellite Oceanography
Primary Production
Model

Océanographie Satellitaire
Production Primaire
Modèle

Nicolas HOEPFFNER ^a, Trevor BARKER ^a, Leo NYKJAER ^a,
Maita ESTRADA ^b, Peter SCHLITTENHARDT ^a

^a Institute for Remote Sensing Applications, Joint Research Centre of the European Communities, I-21020 Ispra (Va), Italy.

^b Instituto de Ciencias del Mar, Consejo Superior de Investigaciones Cientificas Paseo Joan de Borbo, s/n, 08039 Barcelona, Spain.

Received 22/10/93, in revised form 26/04/94, accepted 3/05/94.

ABSTRACT

Spectral models of solar irradiance in the atmosphere and underwater are combined with satellite ocean colour data to determine the water column integrated daily rate of primary production in an upwelling centre off the coast of Mauritania. The local algorithm of primary production is based on first principles of photosynthetic physiology in marine algae, and accounts for some optical characteristics of the atmosphere over various marine environments. The results (integrated daily rate of primary production) are shown for different computational schemes, including the segmentation of the studied area into several provinces, each of them having a proper set of bio-optical and meteorological parameters. Some examples are given to illustrate the validation of the model results with other *in situ* and theoretical studies in the same area.

RÉSUMÉ

Utilisation d'un modèle analytique pour déterminer la production primaire intégrée à partir de données satellitaires dans une région de remontée d'eau

Des données de couleur océanique obtenues par satellite (CZCS) sont intégrées dans un modèle spectral semi-analytique visant à déterminer la production journalière intégrée dans une région de remontée d'eau au large des côtes mauritaniennes. La production primaire locale est déterminée à partir des premiers principes de la physiologie photosynthétique chez les algues marines. De plus, le modèle tient compte de la variabilité des caractéristiques optiques de l'atmosphère au-dessus de régions océaniques différentes. Les résultats de production primaire (en $\text{gC}\cdot\text{m}^{-2}\cdot\text{j}^{-1}$) sont présentés pour différentes techniques de calcul, avec soit un schéma homogène de distribution des paramètres bio-optiques et météorologiques dans la zone étudiée, soit une division de cette zone en plusieurs provinces bio-géochimiques ayant leurs propres paramètres. Une étude comparative avec des mesures *in situ* et des modèles semi-empiriques locaux est à la base d'une discussion des résultats en termes de valeurs absolues de production et de sa répartition.

Oceanologica Acta, 1994, 17, 4, 431-442.

INTRODUCTION

For more than a decade, remote sensing techniques have made an important contribution to oceanographic sciences, collecting data on time and space scales much more adequate for global studies than sampling from low speed research ships. Consequently, the number of applications using satellite data, particularly in the visible range, has been growing rapidly (Abbott and Chelton, 1991 and references therein), attributable to the on going development of new algorithms for the calculation of oceanic variables. Among these applications, synoptic mapping of algal pigments at the surface of the oceans (Barale and Schlittenhardt, 1993) has made a reasonable amount of progress, using radiometric data from the Coastal Zone Color Scanner (CZCS), which operated from 1978 to 1986 on board the Nimbus-7 satellite. As a logical continuation, marine primary production by phytoplankton is now accessible from satellite imagery, through various modelling approaches (Eppley *et al.*, 1985; Platt *et al.*, 1988; Campbell and O'Reilly, 1988; Sathyendranath *et al.*, 1989; Morel, 1991).

The efficiency of these models to retrieve water column integrated primary production on a global scale has been recently debated (Balch *et al.*, 1992; Platt and Sathyendranath, 1993). Excluding strictly empirical models, it seems, however, that rational (or semi-analytical) models are, in fact, formulated on similar grounds, and discrepancies that do occur in different studies should be explained in terms of model implementation rather than formulation (Platt and Sathyendranath, 1993). At present, such models have been applied on basin scales, *e.g.* the North Atlantic (Platt and Sathyendranath, 1988; Platt *et al.*, 1991), and the western Mediterranean Sea (Morel and André, 1991). On the other hand, and as pointed out by Balch *et al.* (1992), the performance of these models on regional scales, particularly in dynamic coastal areas, has not yet been investigated, despite the importance of coastal waters in the production of organic carbon (Richards, 1981). Sathyendranath *et al.* (1991) successfully applied a semi-analytical model to retrieve phytoplankton production in the Georges Bank area (western North Atlantic) from satellite data. The authors, however, have focused their study on determining the new production from a local relationship between the surface temperature and the so-called *f*-ratio.

The aim of this paper is to test an existing deterministic model to evaluate the daily rate of primary production from satellite data, in a region off the coast of Mauritania. This area is characterized by strong dynamics associated with upwelling features along the coast, yielding high productivity throughout most of the year. Economically important, this region has been extensively visited by research vessels, as part of the international programme "Cooperative Investigation of the Northern part of the Eastern Central Atlantic" (CINECA; Hempel, 1982). This notwithstanding, Bricaud *et al.* (1987) showed, using satellite data, evidences of an underestimation of primary production in this region, due to the offshore extension of mesotrophic waters which could not be detected from ship cruises.

In this work, the implementation of a semi-analytical model described by Platt and Sathyendranath (1988) is modified to account for specific marine and atmospheric dynamics in coastal environments. This model uses ocean colour data to determine primary production through a physiological relationship linking phytoplankton photosynthesis to light. Such a mechanistic approach has the advantage of maintaining a uniform precision throughout its wide range of applicability. The results are then compared with data obtained from a site-specific model (Bricaud *et al.*, 1987), which uses empirical formulations that, possibly, improve the precision of the model, but restrict its range of applicability because of the natural variabilities in time and space of oceanic processes.

CONCEPTUAL MODELLING OF PRIMARY PRODUCTION FROM SPACE

The protocol, used in this work, to estimate marine productivity from satellite data is based on the model of Platt and Sathyendranath (1988), which relies on the assumption that algal photosynthesis in the oceans is mainly controlled by the flux of photons and the amount of algal pigments that absorbs them.

As shown in Figure 1, the biomass (*i.e.*, concentration of chlorophyll-like pigment) is obtained from CZCS ocean colour data; the values are then combined with atmospheric and underwater light field data in a well-known equation, which formulates the dependence of the photosynthetic rate on the available light, the so-called P-I curve. This relationship can be expressed as (Platt and Sathyendranath, 1991):

$$P_{(z,t,\lambda)} = B_{(z)} P_m^B \left(1 - \exp \left[- \left(\alpha^B I_0 \sin \left(\frac{\pi t}{D} \right) e^{-Kz} \right) / P_m^B \right] \right), \quad (1)$$

where the instantaneous rate of photosynthesis at each depth z , and wavelength λ , depends on the biomass $B_{(z)}$, the photosynthetic parameters (P_m^B) and (α^B) characterizing the P-I curve, and the surface irradiance at local apparent noon. The diurnal variation of irradiance at the ocean surface is expressed by a first-order sinusoid, whereas the term $\exp(-Kz)$ accounts for the modification of light as it penetrates the water column, with K being the optical attenuation coefficient.

MODEL COMPUTATION

A solution of (1) requires several computational steps to determine the irradiance just below the sea surface, the biomass profile, the photosynthetic parameters, the parameters of underwater light transmission, and lastly the daily rate of water column production. At each of these steps, the model allows for various degrees of complexity to estimate the parameters (Platt *et al.*, 1991; Kyewalyanga *et al.*, 1992).

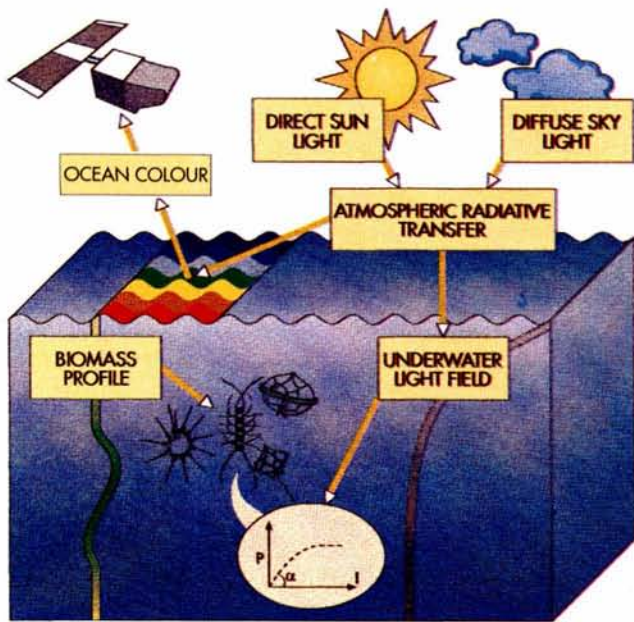


Figure 1

Conceptual diagram of a semi-analytical model to determine primary production in marine waters from satellite data. Such a concept is applied to a region off the northwest coast of Africa.

Schéma conceptuel d'un modèle semi-analytique visant à déterminer la production primaire océanique à partir des données satellitaires. Un tel concept est appliqué à une région de remontée d'eau de la côte nord-ouest africaine.

Biomass retrieval

The method to determine chlorophyll concentrations in the water column is taken from Sathyendranath and Platt (1989). Briefly, the biomass, $B_{(z)}$, at each depth in a vertically homogeneous water column is directly obtained from a satellite-weighted surface estimate, following a method described by Gordon and Clark (1980). In the case of a subsurface chlorophyll maximum, inaccessible to satellite sensors, a theoretical profile is assumed and defined by three parameters of a Gaussian distribution superimposed on a background chlorophyll value, B_0 , (Platt *et al.*, 1988):

$$B_{(z)} = B_0 + \frac{h}{\sigma\sqrt{2\pi}} \exp\left[-\frac{(z - z_m)^2}{2\sigma^2}\right], \quad (2)$$

where the parameters, σ , h , and z_m identify the width, the total biomass above background, and the position of the Gaussian profile, respectively. Sathyendranath and Platt (1989) showed that a combination of two parameters, *i.e.* the sum of peak height and background concentration, $B_0 + h / [\sigma\sqrt{(2\pi)}]$, can be derived from the blue-green reflectance ratio obtained from CZCS data. Consequently, the model implementation using satellite data is reduced to the knowledge of five biological parameters: three associated with the biomass profile (z_m , the position of the chlorophyll maximum; σ , the width of the chlorophyll maximum; and ρ , the ratio of the peak height to the background chlorophyll concentration) and two photosynthetic parameters.

Surface light field

Direct and diffuse irradiances at sea surface are computed in Platt and Sathyendranath (1988) from a model of radiative transfer in the atmosphere developed by Bird (1984) for continental areas. Following a similar approach, we have used an updated version of Bird's model (Bird and Riordan, 1986), further modified by Gregg and Carder (1990) to account for the variability of some atmospheric components over various marine environments. Major changes, when compared with the model of Platt and Sathyendranath (1988), occur in the computation of aerosol transmittance which can be expressed as:

$$T_a(\lambda) = \exp[-\beta\lambda^{-\alpha}M(\theta)], \quad (3)$$

where the Angstrom exponent, α , and the turbidity coefficient, β , are related to the aerosol size distribution and to the aerosol concentration, respectively. These parameters are estimated from a Junge approximation of Gathman's marine aerosol model (Gregg and Carder, 1990) which assumes three size classes of particles: a background continental-type of aerosols with a mean radius of $0.03 \mu\text{m}$, a sea-spray component with a mean radius of $0.24 \mu\text{m}$, and an episodic component of larger particles (mean radius = $2.0 \mu\text{m}$). The term $M(\theta)$ in (3) refers to the air mass, computed as in Bird and Riordan (1986). Also, the reflectance at the air-sea interface is modified by Gregg and Carder (1990) to account for the wind field responsible for sea-spray particles and sea-foam reflectance.

In this work, the ozone transmittance, $T_o(\lambda)$, was calculated using the Van Heuklon (1979) formulation to estimate the ozone scale heights, O_3 , as a function of location (Lat. and Long.) and the day number (DN):

$$O_3 = 235 + \{ 150 + 40 \sin [0.9865 (DN - 30)] + 20 \sin [3 (Long.)] \} [\sin^2 (1.28 Lat.)]$$

and,

$$T_o(\lambda) = \exp[-M_o(\theta)O_3a_o(\lambda)], \quad (4)$$

where $M_o(\theta)$ is the ozone mass computed as in Gregg and Carder (1990), and $a_o(\lambda)$ is the ozone absorption coefficient given from standard tables (*e.g.* in Gregg and Carder, 1990).

The amount of precipitable water, w , necessary to correct the water vapour transmittance, $T_w(\lambda)$, was estimated using Leckner's method as given by Iqbal (1983), as a function of the relative humidity, RH , and the air temperature, T :

$$w = \left[0.493RH \exp\left(26.23 - \frac{5416}{(T + 273)}\right) \right] / (T + 273)$$

and,

$$T_w(\lambda) = \exp\left[\frac{-0.2385a_w(\lambda)wM(\theta)}{[1 + 20.07a_w(\lambda)wM(\theta)]^{0.45}} \right], \quad (5)$$

from Gregg and Carder (1990).

Rayleigh scattering and absorption due to other mixed gases (including oxygen) are computed according to Bird and Riordan (1986). Changes in the atmospheric path-length (or air mass), $M(\theta)$, due to differences in the air

pressure, were neglected as they do not significantly affect the model (Gregg and Carder, 1990).

Also, the reflectance at the air-sea interface is computed separately for the direct and diffuse irradiance, and accounts for three possible sea states. For a flat ocean (wind speed < 4 m.s⁻¹), reflectance is directly computed from Fresnel's law, whereas in other cases (wind speed between 4 and 7 m.s⁻¹, and higher than 7 m.s⁻¹) a foam reflectance due to surface roughness is added to the computation following the protocol recommended by Gregg and Carder (1990).

Thus, the model of Gregg and Carter (1990) represents an improvement in the determination of primary production in the oceans from remotely sensed data. Its utilization, however, requires the knowledge of additional parameters to define the atmospheric environment over the area of study. These parameters are, namely, the instantaneous and 24 h. – averaged wind speed, the airmass type, the relative humidity, the visibility and the air temperature.

Underwater light field

A spectral model (Prieur and Sathyendranath, 1981; Sathyendranath and Platt, 1988) is used for the computation of light energy, from 400 to 700 nm, just below the sea surface and at various depths in the euphotic layer. The vertical attenuation coefficient for the direct, $K_d(\lambda)$, and diffuse, $K_s(\lambda)$, components of irradiance were calculated accounting for the angular distribution of the light field just below the surface, θ' is the sun zenith angle in water, and μ is the mean cosine for diffuse sky light after refraction at a flat sea surface:

$$K_d(\lambda) = \frac{[a_t(\lambda) + b_w(\lambda)]}{\cos(\theta')}, K_s(\lambda) = \frac{[a_t(\lambda) + b_w(\lambda)]}{\bar{\mu}}, \quad (6)$$

We have neglected multiple scattering effects, although Sathyendranath and Platt (1991) have observed significant differences in the depth of the euphotic zone due to this effect. Attenuation coefficients are obtained by assuming a negligible contribution due to mineral particles. This assumption would be difficult to justify for very near shore waters. In this case, however, the error in K on the final result will still be much smaller than that associated with the satellite algorithm to determine chlorophyll concentration in "case 2 waters" (60% – 100%, B. Sturm pers. comm.). Then, the total absorption, $a_t(\lambda)$, and backscattering coefficients, $b_{bt}(\lambda)$, can be written as:

$$a_t(\lambda) = a_w(\lambda) + a_{ph}(\lambda) + a_y(\lambda),$$

$$b_{bt}(\lambda) = \tilde{b}_{bw} b_w(\lambda) + \tilde{b}_{bph} b_{ph}(\lambda), \quad (7)$$

where the subscripts w , ph , and y refer to water molecules, phytoplankton, and yellow substance, respectively. The term \tilde{b}_b represents the backscattering to total scattering ratio. Absorption and scattering properties of molecular water are taken from Morel (1974), whereas absorption by yellow substance is derived from Prieur and Sathyendranath (1981) who have assumed that $a_y(440)$ is 20% of the total absorption coefficient of seawater. From Sathyendra-

nath and Platt (1988), the spectral absorption by phytoplankton can be written as:

$$a_{ph}(\lambda) = B_{(c)} \frac{0.355}{(6.103 + B_{(c)})} a_{ph}^{*'}(\lambda), \quad (8)$$

where $a_{ph}^{*'}(\lambda)$ is an averaged absorption spectrum of phytoplankton and normalized at 440 nm. Knowing $a_{ph}(\lambda)$, the phytoplankton backscattering can be calculated using the attenuation coefficient at 550 nm, ($c_{ph} = a_{ph} + b_{ph}$), and the formulation given by Morel (1980) for $b_{ph}(550)$:

$$b_{ph}(\lambda) = [a_{ph}(550) + 0.12B_{(c)}^{0.63}] - a_{ph}(\lambda) \quad (9)$$

The computation of (9) required the assumption of c_{ph} being independent of wavelength as suggested by Bricaud *et al.* (1983) from the spectral complementarity between $a_{ph}(\lambda)$ and $b_{ph}(\lambda)$. On the other hand, a value of 1% has been taken for the backscattering to total scattering ratio of phytoplankton and associated detrital particles, as deduced from the range of values observed in the upwelling area off Mauritania (Bricaud *et al.*, 1983). Note that most of the formulations to determine the inherent optical properties of various constituents in seawater were established from data collected in different marine regions, including the upwelling system of Northwest Africa (Morel and Prieur, 1976; Prieur and Sathyendranath, 1981).

SATELLITE CHLOROPHYLL DATA

Pre-processed CZCS data were taken from the receiving station at Maspalomas in the Canary Islands. Electromagnetic signals were calibrated taking into account the sensitivity loss of the sensor, as evaluated by Sturm (1986) on clear water pixels from 53 orbits ranging from November to October 1985. The atmospheric effects on the water-leaving radiances were evaluated according to André and Morel (1991). In a first step, the reflectance of seawater was retrieved after corrections for Rayleigh scattering (Gordon *et al.*, 1988) and for atmospheric attenuation of the upwelled signal. These values were, in a second step, corrected for aerosol scattering, using an iterative calculation of the reflectances on each pixel. This latter procedure permits differentiation between case 1 waters with low chlorophyll concentration (< 2.0 mg.m⁻³), case 1 waters with high chlorophyll concentration (> 2.0 mg.m⁻³), and case 2 waters dominated by non-chlorophyllous particles. The threshold between case 1 and case 2 waters is based on the subsurface reflectance signal (R_s) in channel 3 of CZCS (Bricaud and Morel, 1987). The algorithms to retrieve chlorophyll concentrations from CZCS ocean colour data are as follows, for case 1 waters:

$$\ln C = 0.768 - 2.61 X_1 + 0.791 X_1^2 - 0.338 X_1^3, \quad \text{for } C < 2.0 \text{ mg.m}^{-3}$$

$$\ln C = 1.476 - 8.196 X_2 + 6.951 X_2^2 - 23.547 X_2^3, \quad \text{for } C > 2.0 \text{ mg.m}^{-3}$$

and for case 2 waters :

$\ln C = 0.334 - 1.68 X_1$, for $R_s(\lambda_3) < R'_s(\lambda_3)_{lim}$

$\ln C = 1.31 - 3.674 X_2$, for $R_s(\lambda_3) > R'_s(\lambda_3)_{lim}$
with,

$$R_s(\lambda_3)_{lim} = 0.01 \exp [1.05 - 0.02 X_1 - 0.429 X_1^2 + 0.094 X_1^3]$$

$$R'_s(\lambda_3)_{lim} = 0.01 \exp [-3.58 + 0.675 X_2 - 3.77 X_2^2 - 3.43 X_2^3]$$

where X_1 depends on the reflectance ratio of CZCS band 1 to band 3, $X_1 = \ln [R(\lambda_1) / R(\lambda_3)]$, whereas X_2 depends on the reflectance ratio of CZCS band 2 to band 3, $X_2 = \ln [R(\lambda_2) / R(\lambda_3)]$. The algorithm for case 2 waters was developed from Morel (1988)'s case 1 model (B. Sturm, pers. comm.).

For any water pixel, the iterative process starts by assuming that it belongs to case 1 water with low chlorophyll concentration. The processing of satellite data has been carried out using software developed at the Institute for Remote Sensing Applications of the European Communities Joint Research Centre. The software was then integrated in the widely distributed ERDAS image processing package. Details on the development of algorithms can be found in Sturm (1993).

FIELD DATA

Phytoplankton biomass

The vertical structure of chlorophyll was obtained from a Spanish cruise "ATLOR VII" of the R/V *Cornide de Saavedra* along the northwest African coast in November 1975 (Estrada, 1980). A total of 35 stations were visited between latitudes 17°N and 23°N to collect water samples at standard depths. Stations were distributed along the coast, as well as along cross-shelf transects at 21°N, 20°N, and 19°N of latitude, with offshore stations located as far as 22°W of longitude. Primary production was also measured using the ^{14}C uptake technique on deck-incubated samples. Hourly rates of photosynthesis were transformed into daily rates using factors obtained experimentally during the cruise (Estrada, 1980). Because of the rather poor vertical resolution of these chlorophyll measurements, we completed this data set by using chlorophyll profiles made recently during the French cruise "EUMELI 5" in December 1992 (Lantoiné and Neveux, unpubl. data). During this cruise, more accurate chlorophyll profiles were monitored for coastal and shelf-break waters (bottom depth < 2000 m), slope waters (2000 m < bottom depth < 4000 m), and open-ocean waters (bottom depth > 4000 m) in the vicinity of our studied area.

Photosynthetic parameters

To our knowledge, a data set covering the photosynthetic parameters of phytoplankton was not available for the area and time period of the study. As an alternative, the assimilation number at saturated light intensity, (P_m^B), was evaluated from an empirical relationship developed by Minas *et al.*

(1982) from the concentrations of nitrate and chlorophyll-*a* in the northwest African upwelling system. On the other hand, Platt *et al.* (1992) have recently showed evidence of a nutrient control of photosynthesis during bloom episodes in the Sargasso Sea. In their study, the efficiency of photosynthesis in limited light, α^B , can be related to (P_m^B) within the range 0-12 mgC (mg Chl a) $^{-1}$ h $^{-1}$. Since a similar range of P_m^B values was obtained in the northwest African upwelling (Minas *et al.*, 1982), we have assumed that the relationship between both photosynthetic parameters as suggested in the figure 3a (surface data) of Platt *et al.* (1992) is also valid for our studied area. We realize, however, that the environmental conditions that can affect directly the magnitude of α^B (nutrient concentration, light,...) can differ considerably between both locations, the African upwelling center and the Sargasso Sea. In the present study, the concentrations of nitrate in the upwelling area were also taken from the cruise "ATLOR VII" (Manriquez and Fraga, 1978).

Meteorological data

Relative humidity, air temperature, visibility, and wind field are the atmospheric data relevant to the model. Part of these data was taken from the cruise "ATLOR VII" (A. Juliá, pers. com.) and averaged over the entire cruise period to constitute a typical atmosphere of the studied area, in November. The wind field, however, was retrieved from the European Centre for Medium-range Weather Forecasts (ECMWF, Reading, U.K.), giving *u*- and *v*- components of the wind at 10 m height on a spatial grid of 1.875 degrees in coordinates. Averaged and instantaneous wind data were retrieved for the same date as the CZCS chlorophyll image.

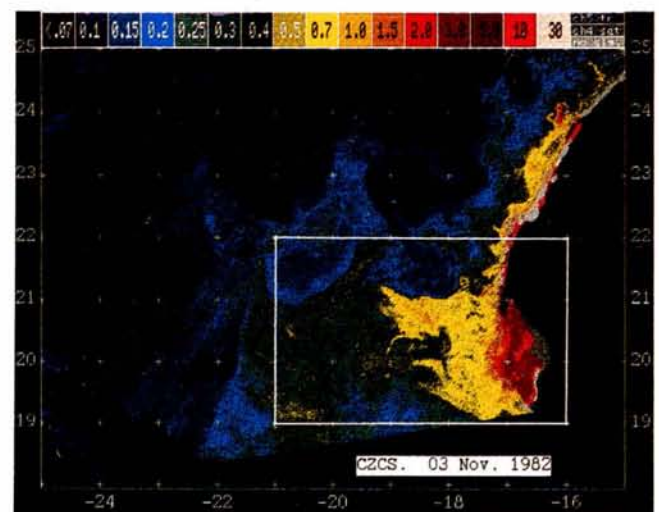


Figure 2

Surface chlorophyll concentration (in $\text{mg}\cdot\text{m}^{-3}$) off the coast of Mauritania, as perceived by the CZCS ocean colour sensor on 3 november 1982. The enclosed area is studied for primary production.

Concentration de chlorophylle en surface (en $\text{mg}\cdot\text{m}^{-3}$) au large de la Mauritanie et obtenue à partir de la sonde CZCS le 3 novembre 1982. L'encadré sur la figure correspond à la zone d'étude de production primaire.

RESULTS

Chlorophyll distribution

The area of interest lies approximately between latitudes 19°N and 23°N, and between the coastline and 22°W of longitude. This region is known to exhibit permanent upwelling, the magnitude of which varies, however, with the time of the year (Mittlestaedt, 1991), reaching a maximum activity in spring and a minimum in September. Another peculiarity of this region resides in the distribution of water masses. A major front is usually observed around the latitude of Cape Blanc (*ca.* 21°N), and separates North Atlantic Central Water (NACW) from South Atlantic Central Water (SACW), (Hagen and Schemainda, 1987). These water masses, originally located at intermediate depth, constitute most of the upwelled waters along the coast. North of Cape Blanc, relatively warm, salty and low-nutrient NACW will dominate at the surface, while cooler, fresher and nutrient-rich SACW will prevail in the upwelling area south of Cape Blanc (Minas *et al.*, 1982).

Figure 2 shows the chlorophyll distribution from CZCS in the area of study in November, which corresponds to a period of intermediate upwelling strength (Bricaud *et al.*, 1987). An apparent feature can be observed in the form of a "giant filament" of high chlorophyll concentration ($0.7 - 1.5 \text{ mg.m}^{-3}$), located south of Cape Blanc and extending far offshore. Such a feature is not uncommon in this area (Bricaud *et al.*, 1987), and results from the convergence at the surface of the southward Canary Current and the poleward Counter Current (Mittlestaedt, 1991), carrying upwelled coastal water as far as 300-400 km offshore at the latitude of Cape Blanc. The satellite image (Fig. 2) also reveals sharp discontinuities between open ocean waters ($0.1 - 0.2 \text{ mg Chla. m}^{-3}$), north of Cape Blanc, and coastal waters expended offshore south of 21°N. Some interleavings between both water types produce spectacular mesoscale eddies which are of importance in dividing the area into a set of biologically independent provinces. The highest chlorophyll biomass ($\text{Chla} > 10 \text{ mg. m}^{-3}$) is concentrated within a narrow band along the coast, limited offshore by the 50 m isodepth line, including the "Banc d'Arguin" area south of Cape Blanc. This area of high biomass concentration has been qualified from the computation as case 2 waters and, therefore, the absolute values of chlorophyll concentration should be interpreted with caution, since the algorithm for case 2 waters was originally developed for the Adriatic Sea (B. Sturm, pers. comm.). Nevertheless, high phytoplankton biomass ($\text{Chla} > 20 \text{ mg.m}^{-3}$) has often been observed from *in situ* measurements in the region of "Banc d'Arguin" (Estrada, 1980; Minas *et al.*, 1982).

At discrete locations during the cruise "ATLOR VII", chlorophyll values in November 1975 at the surface (Estrada, 1980) were comparable to those recorded for the same period by the CZCS sensor within the area surrounding those local points, although a 7-year period separates both data set. Figure 3 summarizes chlorophyll and nitrate values along two long cross-shelf transects at 20°N and 21°N, and a shorter one as 22°N. Although the high temporal variability of oceanic processes in coastal waters inhi-

bits considerably the interpretation of instantaneous cruise data, a trend of increasing values of nitrate and chlorophyll concentrations can be observed as one approaches the shelf break. At this point, differences occur between both long transects, with higher nitrate and lower chlorophyll concentrations at 21°N than at 20°N. Intermediate concentrations of both variables were measured at 22°N.

Bio-geochemical provinces

One approach to computing primary production using equation (1) is to subdivide the area of study into provinces (Platt and Sathyendranath, 1988), in each of which the bio-optical parameters relevant to the model are assumed to remain constant for a given time period. As mentioned earlier, these parameters refer to photosynthesis-light curves and biomass profiles.

It is clear from the chlorophyll map (Fig. 2) that the upwelling activity, north of Cape Blanc (21°N), is concentrated mainly over the shelf and upper slope regions, as indicated by high biomass values. This region is limited offshore by the 200 m depth line. South of 21°N, this situation is probably still valid but the chlorophyll distribution appears distorted by the surface water dynamics in this area. Accordingly, the area of study (inserted box in Fig. 2) was divided into five provinces (Fig. 4), including:

1) a narrow band from the coast line to 50 m isopleth, covering most of the turbid case 2 waters;

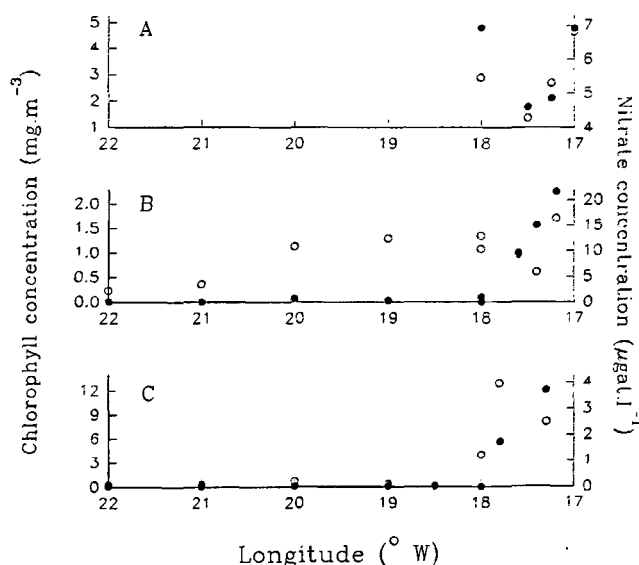


Figure 3

Nitrate (filled circle) and chlorophyll (open circle) concentrations at three transects perpendicular to the Mauritanian coast; (A) at 22°N, (B) at 21°N, and (C) at 20°N of latitude. Data were collected during the Spanish cruise "Atlors VII" of the R/V Cornide de Saavedra in november 1975.

Distribution des nitrates (cercle plein) et chlorophylle (cercle vide) le long de trois sections perpendiculaires à la côte mauritanienne aux latitudes : (A) 22°N, (B) 21°N et (C) 20°N. Les données de terrain ont été prises lors de la mission espagnole « Atlor VII » sur le *Cornide de Saavedra* en novembre 1975.

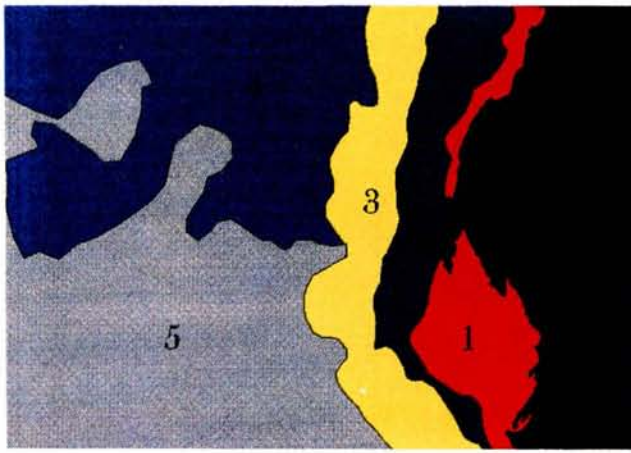


Figure 4

Identification of the biogeochemical provinces in the area off the coast of Mauritania. The selection is based on the bathymetry (50 m, 200 m and 2000 m depth lines) and the structure of surface currents (see text for details).

Identification des provinces bio-géochimiques dans une région de remontée d'eau au large des côtes mauritaniennes. La sélection repose sur une étude bathymétrique (lignes des 50 m, 200 m et 2000 m) et sur la structure des courants en surface (voir texte).

2) the shelf break area between 50 m and 200 m depth lines, where NACW and SACW are upwelled at the surface;

Table 1

Selected values of the biological and meteorological parameters required by the model for each bio-chemical provinces as shown in Figure 4.

Données biologiques et météorologiques nécessaires à l'utilisation du modèle de production pour chacune des provinces bio-géochimiques représentées sur la figure 4.

Parameters	Bio-geochemical provinces					
	1	2	3	4	5	
Biomass profile	z_m (m)			85		
	σ (m)	Uniform	Uniform	Uniform	18	Uniform
	ρ				2.3	
Photosynthetic parameters	P_m^B (mgC.mg Chla ⁻¹ .h ⁻¹)	1.5	7.3	7.3	4.5	4.5
	α^B (mgC.mg Chla ⁻¹ .(W.m ⁻²).h ⁻¹)	0.03	0.07	0.07	0.05	0.05
Atmospheric conditions	Airmass type	10	7	5	1	1
	Mean wind speed over 24 h (m.s ⁻¹)	4.1	4.1	4.05	3.8	4.4
	Instantaneous wind speed (m.s ⁻¹)	4.68	4.36	4.53	4.3	5.1
	Relative humidity (%)	80	80	80	80	80
	Visibility (km)	15	20	20	25	25
	Air temperature (°C)	17	17	17	17	17

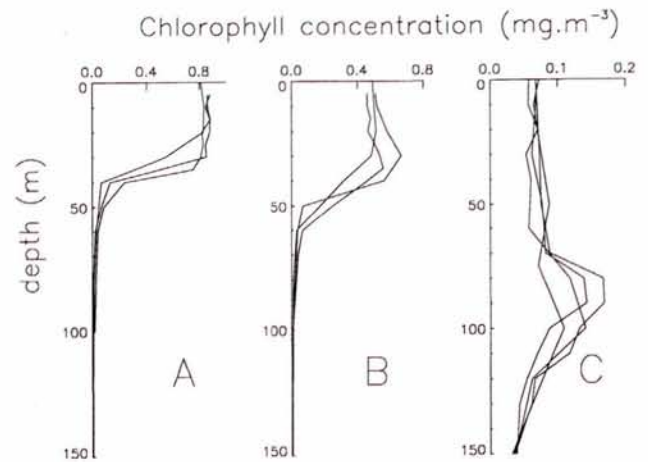


Figure 5

Chlorophyll profiles at different stations in (A) the eutrophic (~ 20°30N; 18°35W), (B) the mesotrophic (~ 18°30N; 21°05W) and (C) the oligotrophic (~ 21°00N; 31°10W) sites of the French cruise "EUMELI V".

Profil de chlorophylle à différentes stations dans les sites (A) eutrophe (~ 20°30N; 18°35W), (B) mésotrophe (~ 18°30N; 21°05W) et (C) oligotrophe (~ 21°00N; 31°10W) du programme français « EUMELI V ».

3) an area between the 200 m and 2000 m depth lines, which can be seen as a transient zone between open ocean and upwelled waters;

4) and finally, offshore waters were divided into a northern (region 4) and southern (region 5) part by digitizing the distinct chlorophyll patterns observed in Figure 2, which result from surface current dynamics.

The biological and meteorological parameters that were assigned to each province are shown in Table 1. In most of the provinces, we have assumed a homogeneous vertical profile of chlorophyll. This is undoubtedly the case in regions 1, 2, and 3, where upwelling activity, meteorological forcing, and shallow bottom depth all contribute to an uniform distribution of biological variables in the euphotic layer. In offshore waters (regions 4 and 5), a subsurface maximum of chlorophyll could occur as a result of a stratification of the water column. Chlorophyll profiles taken during the cruise EUMELI 5 in December 1992 within, or in the vicinity of, our studied area are represented in Figure 5. In the first two cases (Fig. 5A and B), surface concentrations ranged between 0.6 and 0.8 mg Chla m⁻³, similar to values observed by Estrada (1980) along a transect at 21°N, and similar to concentrations retrieved from CZCS data (Fig. 2) in region 5. The vertical profiles of chlorophyll at these two locations (Fig. 5A and B) are quasi-uniform within the euphotic layer which is, on average, restricted to the first 40-50 m at these two stations (P.F.O. report, 1989). This result, corroborating the strong physical processes occurring in offshore waters south of 21°N, motivated us to assume a vertically-uniform distribution of chlorophyll in the entire region 5. On the other hand in Figure 5C, chlorophyll profiles present a distinct subsurface maximum at 80 – 90 m, representative of oligotrophic "blue" waters. At the surface, the concentration of chlorophyll averages 0.16 mgChla.m⁻³, in agreement with CZCS data in

region 4 ($0.1\text{--}0.2 \text{ mgChla}\cdot\text{m}^{-3}$). The vertical distribution of chlorophyll in region 4 was then approximated as a Gaussian distribution with parameters given in Table 1, estimated from the profiles in Figure 5C.

Large-scale estimates of primary production are also sensitive to the values of α^B and P_m^B assigned to each of the provinces. However, the scarcity of photosynthesis light measurements in the studied area limits considerably the model's implementation with exact values of these parameters, and bound our choice of α^B and P_m^B to several assumptions. In region 1, nitrate concentrations in the water were not known and, thus, the assimilation number P_m^B (Table 1) was taken from Table 2 of Minas *et al.* (1982) for situations where chlorophyll concentrations are higher than $10 \text{ mg Chla}\cdot\text{m}^{-3}$. These values range from 1.3 to $1.9 \text{ mgC}\cdot(\text{mgChla})^{-1}\cdot\text{h}^{-1}$, and a mean value of $1.5 \text{ mgC}\cdot(\text{mgChla})^{-1}\cdot\text{h}^{-1}$, was used here.

In regions 2 and 3, our evaluation of P_m^B was also obtained from table 2 of Minas *et al.* (1982) by averaging values for three different situations suggested in Figure 3 from the concentrations of chlorophyll and nitrate: north of 21°N , concentrations of nitrate and chlorophyll (Fig. 3a), range from 1 to $10 \mu\text{gat}\cdot\text{l}^{-1}$ and from 5 to $10 \text{ mg}\cdot\text{m}^{-3}$, respectively, suggesting a P_m^B value of $3.2 \text{ mgC}\cdot(\text{mgChla})^{-1}\cdot\text{h}^{-1}$ from the classification proposed by Minas *et al.* (1982); at 21°N (Fig. 3b), concentrations of chlorophyll are lower than the previous situation ($< 5 \text{ mg}\cdot\text{m}^{-3}$), whereas the concentrations of nitrate are higher than $10 \mu\text{gat}\cdot\text{l}^{-1}$, resulting in a P_m^B value of $11.8 \text{ mgC}\cdot(\text{mg Chla})^{-1}\cdot\text{h}^{-1}$; finally, south of 21°N (Fig. 3c), chlorophyll concentrations remain less than $5 \text{ mg}\cdot\text{m}^{-3}$ for a range of nitrate of $1\text{--}10 \mu\text{gat}\cdot\text{l}^{-1}$, corresponding to a P_m^B value of $7.1 \text{ mgC}\cdot(\text{mgChla})^{-1}\cdot\text{h}^{-1}$ (Minas *et al.*, 1982). From these results, a mean value of $P_m^B = 7.3 \text{ mgC}\cdot(\text{mgChla})^{-1}\cdot\text{h}^{-1}$ was then taken as representative of regions 2 and 3.

The efficiency of photosynthesis in weak light, α^B , in regions 1 to 3 (Tab. 1), was then approximated from the value of P_m^B and the relationship between both parameters suggested by Platt *et al.* (1992) in their Figure 3a (data from the upper 20 m of the water column).

Table 2

Averaged values of water column integrated daily rate of phytoplankton photosynthesis in an upwelling region off the coast of Mauritania. To allow comparative with the semi empirical model of Bricaud et al. (1987), the area has been divided in sectors north and south of 21°N .

Valeurs moyennes de production primaire journalière intégrée, dans une région au large des côtes mauritaniennes. Par souci d'une comparaison avec les résultats d'un modèle semi-empirique de Bricaud *et al.* (1987), la région a été divisée en secteurs nord et sud de la latitude 21°N .

	North of 21°N	South of 21°N
Bricaud <i>et al.</i> (1987)	0,86	1,34
Present Data		
Homogeneous case	0,85	1,2
Biogeochemical provinces	0,75	1,1

In open ocean waters (regions 4 and 5), the classification proposed by Minas *et al.* (1982) is no longer valid since the concentrations of nitrate are usually lower by one or two orders of magnitude than in coastal and slope upwelling waters. However, the situation would be similar to a non-blooming open-ocean regime. Using offshore stations of the cruise "ATLOR VII" (see also Fig. 3), Manriquez and Fraga (1978) observed concentrations of nitrate in the order of $0.3 \mu\text{gat}\cdot\text{l}^{-1}$, or lower, in the productive layer, similar to what is observed in the Sargasso Sea (excluding the spring period) by Platt *et al.* (1992). Therefore, a typical value of $\alpha^B = 0.05 \text{ mgC}\cdot(\text{mgChla})^{-1}\cdot\text{h}^{-1}\cdot(\text{W}\cdot\text{m}^{-2})^{-1}$, as suggested by Platt *et al.* (1992) for this situation, has been used in this work for regions 4 and 5. An equivalent P_m^B value of $4.5 \text{ mgC}\cdot(\text{mgChla})^{-1}\cdot\text{h}^{-1}$ was also derived from Platt *et al.* (1992).

As mentioned earlier, some of the atmospheric parameters were directly averaged from log-ship data of the cruise "ATLOR VII" in November 1975. Exception is for the "airmass type" (Tab. 1) which is included in the determination of irradiance at sea surface from the model of Gregg and Carder (1990). This quantity varies from 1 to 10 depending on the location of the studied area. A value of 10 has been selected for the near-coastline region (*i.e.*, region 1 in Fig. 4) progressively decreasing to 1, a typical value for open ocean waters. Also, relative humidity and visibility could not be assessed from the cruise report available; we have thus assumed reasonable values of these parameters under marine conditions. The reduction of visibility toward the coast (see Tab. 1) is to account for an increase in evaporation and moisturization of the atmosphere as one approaches the coastline.

Integrated daily rate of photosynthesis

For each pixel of chlorophyll data from CZCS, the vertical profile of biomass was estimated and the primary production was calculated from (1) every half hour, at a vertical resolution of 1m, and at 61 wavelengths. Results were then integrated over the entire daylight period (assuming clear-sky conditions), over the euphotic layer (limited at depth to the 1% light level), and over the Photosynthetic Active Radiation (PAR, ranging from 400 to 700 nm).

On a first run (Fig. 6A), the model of marine productivity has been tested without differentiation of bio-geochemical provinces. A uniform biomass profile was assumed everywhere in the area of investigation, and directly obtained from CZCS estimates. The photosynthetic parameters were set at constant values: $\alpha^B = 0.05 \text{ mgC}\cdot(\text{mgChla})^{-1}\cdot\text{h}^{-1}\cdot(\text{W}\cdot\text{m}^{-2})^{-1}$, and $P_m^B = 5.0 \text{ mgC}\cdot(\text{mgChla})^{-1}\cdot\text{h}^{-1}$. Similarly, we have selected constant values for the meteorological parameters with the airmass type fixed at 1 (strictly maritime atmosphere) and visibility at 25 km. The wind speed was taken from ECMWF data at 21°N and 19°W during the period of the CZCS image, and applied to the whole area. Because of such homogeneity in the input parameters, the spatial variability of the integrated primary production is only due to differences in the chlorophyll concentration as seen by satellite. Consequently, the resul-

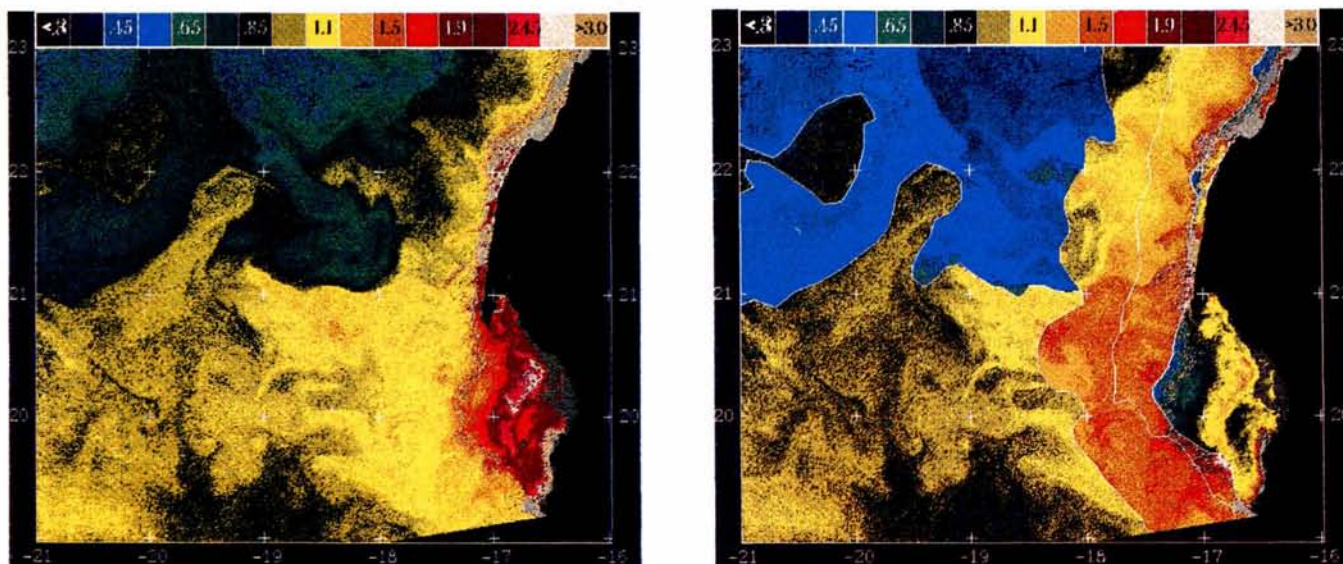


Figure 6

Computed map of the water column integrated daily rate of primary production in the selected region off the coast of Mauritania. (A): the computation assumes all input parameters to remain constant over the entire area. (B): the computation is conducted after segmentation of the studied area into a set of biogeochemical provinces as represented in Figure 4.

Représentation cartographique de la production primaire journalière intégrée dans une région de remontée d'eau au large des côtes mauritaniennes. (A) : Les valeurs de production sont calculées en utilisant des paramètres bio-optiques et météorologiques constants dans la zone d'étude. (B) : Le modèle de production est appliqué en tenant compte des provinces bio-géochimiques représentées en figure 4.

ting productivity map in Figure 6A shows strong similarities with the chlorophyll contours in Figure 2.

Maximum values of primary production ($> 3.0 \text{ gC.m}^{-2}.\text{d}^{-1}$) occur at a few places very close to the coast line, particularly in a region south of 20°N . However, a mean value of $2.0 \text{ gC.m}^{-2}.\text{d}^{-1}$ is more general over the shelf, limited offshore by the 50 m depth line. From there, the daily rate of photosynthesis decreases as one goes further offshore. Note, however, that the production estimates in near shore waters should be interpreted with caution due to higher uncertainties in the CZCS algorithm to retrieve chlorophyll values in case 2 waters. At the shelf-break and slope region (*ca.* between 50 m and 2000 m depth line), production values range from 0.7 to $2.5 \text{ gC.m}^{-2}.\text{d}^{-1}$ with a mean value of $1.1 \text{ gC.m}^{-2}.\text{d}^{-1}$. In open ocean waters, the investigated area is clearly divided into two zones north and south of 21°N , as for the chlorophyll distribution from CZCS data. North of 21°N , a mean value of $0.75 (\pm 0.12) \text{ gC.m}^{-2}.\text{d}^{-1}$ is observed, whereas south of 21°N , higher productivity, $0.97 (\pm 0.1) \text{ gC.m}^{-2}.\text{d}^{-1}$, is obtained as a result of the offshore extension of higher concentration of chlorophyll in this region.

In Figure 6b, the model was applied to our test area after its segmentation into five provinces as described earlier. To each of these provinces were attributed parameters specified in Table 1. The resulting map of primary production differs from that in the previous run, although similarities with the chlorophyll distribution from CZCS are still present.

Over the shelf, primary production displays a wide range of values from 0.4 to $> 3.0 \text{ gC.m}^{-2}.\text{d}^{-1}$, with a mean value of $1.0 \text{ gC.m}^{-2}.\text{d}^{-1}$, lower by a factor of 2 than the value computed in the same area for the homogenous case. Maxima occur just north of 21°N where the upper shelf becomes very nar-

row. At the shelf-break (*i.e.*, between 50 m and 200 m depth line), the daily rate of photosynthesis is on average at its highest value for the entire area of investigation, reaching $1.3 (\pm 0.3) \text{ gC.m}^{-2}.\text{d}^{-1}$ north of 21°N and $1.6 (\pm 0.3) \text{ gC.m}^{-2}.\text{d}^{-1}$ south of 21°N . Also in this case, maximum values occur in the Cape Blanc area (*ca.* 21°N), as well as in a small region south of 20°N . In slope waters (200-2000 m depth line), productivity decreases slightly when compared with values at the shelf break, with a global north-south mean value of $1.27 (\pm 0.15) \text{ gC.m}^{-2}.\text{d}^{-1}$. In regions 2 and 3, P_m^B values vary, according to the classification given in Minas *et al.* (1982), by a factor 3 (3.2 to $11.8 \text{ mgC}(\text{mgChla})^{-1}.\text{h}^{-1}$), and consequently, α^B is also varying. The change in the relative error on the computed production by using these extreme values of P_m^B does not, however, exceed 10% as expected from the sensitivity analyses made by Sathyendranath *et al.* (1989) on a similar production model. Moreover, the error in production estimates increases as P_m^B increases or α^B decreases (Sathyendranath *et al.*, 1989), such that the error due to an increase (or decrease) of both parameters would tend to be even more moderated.

Finally, spatially averaged values of production are the lowest in open ocean waters, with "blue" oligotrophic waters at the north of 21°N being less productive $0.5 (\pm 0.05) \text{ gC.m}^{-2}.\text{d}^{-1}$, than in the giant filament of upwelled waters south of 21°N , $0.95 (\pm 0.07) \text{ gC.m}^{-2}.\text{d}^{-1}$.

MODEL VALIDATION

In situ measurements of primary production conducted in the area of study tend to show higher production at the

shelf-break than at stations near the coastline (Minas *et al.*, 1982). This observation is compatible with the phenomenon of upwelling carrying new nutrients in the illuminated layer at the shelf-break and slope regions (Huntsman and Barber, 1977). Also, a lower efficiency of phytoplankton photosynthesis over the shelf could arise from an effect of self-shading by the phytoplankton cells themselves and non-biogenic particles that contribute significantly to the total suspended matter in these shallow waters. An application of the model described here, assuming homogenous characteristics of seawater and atmosphere in the entire area (see Fig. 6A), is inadequate to simulate such a spatial distribution of primary production. Production values are closely associated with the concentrations of chlorophyll at the surface as observed from satellite, *i.e.*, decreasing from the coastline to offshore waters. However, accounting for bio-geochemical provinces (Fig. 6B), the model yields a better distribution of primary production which is similar to the trend observed from *in situ* measurements.

Around Cape Blanc ($\sim 21^\circ\text{N}$), the continental shelf is at its narrowest and primary production occurs closer to the coastline, as shown by the results of both types of model computations (Fig. 7). Minas *et al.* (1982) reported an averaged value of $2.4 \text{ gC}\cdot\text{m}^{-2}\cdot\text{d}^{-1}$ in the vicinity of Cape Blanc, close to the value obtained in this study, $1.9 - 2.3 \text{ gC}\cdot\text{m}^{-2}\cdot\text{d}^{-1}$. For the same area, Lloyd (1971) observed

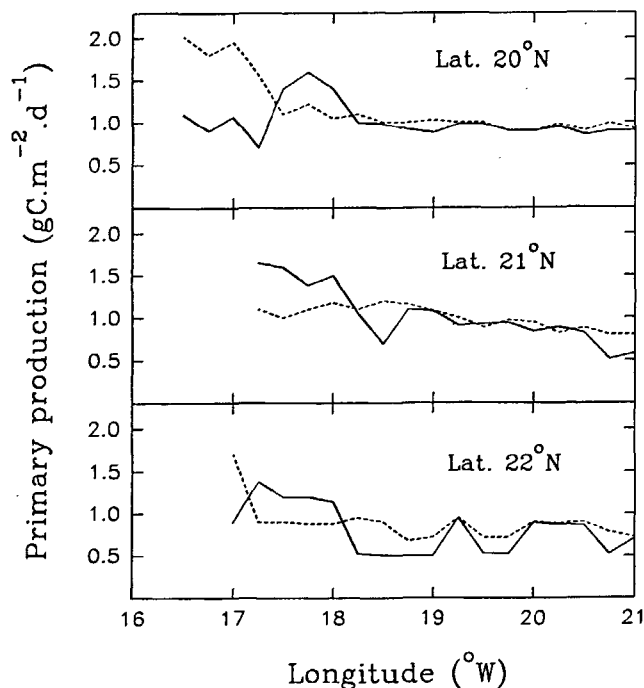


Figure 7

Computed local values of the water column integrated daily rate of primary production along three transects (20°N , 21°N and 22°N). Computed values are represented for the homogeneous case (dotted lines) and after differentiation of biogeochemical provinces (solid lines).

Valeurs calculées de production primaire sur trois sections perpendiculaires à la côte aux latitudes 20°N , 21°N and 22°N . Les valeurs sont représentées pour le cas d'une répartition homogène des paramètres dans la zone d'étude (lignes pointillées) et pour le cas d'une zone divisée en provinces bio-géochimiques (lignes continues).

a daily rate of carbon uptake by phytoplankton between 1.1 and $3.4 \text{ gC}\cdot\text{m}^{-2}\cdot\text{d}^{-1}$ in May and June. Schulz (1982) found somewhat lower mean values, $0.96 - 1.62 \text{ gC}\cdot\text{m}^{-2}\cdot\text{d}^{-1}$, for different period of the year, but at a station already located at the outer shelf off Cape Blanc. South of 21°N , the continental shelf is considerably enlarged to constitute the "Banc d'Arguin" area. Here, the differentiation of bio-geochemical provinces leads to maximum production at the shelf-break (Fig. 7) and slope regions ($17^\circ30'\text{W} - 18^\circ\text{W}$), with values up to $1.7 \text{ gC}\cdot\text{m}^{-2}\cdot\text{d}^{-1}$ along 20°N of latitude. Patches of higher values are observed slightly north and south of 20°N , reaching $2.0 - 2.1 \text{ gC}\cdot\text{m}^{-2}\cdot\text{d}^{-1}$ just off the 50 m depth line. Such high values of primary production in this region have also been observed by Estrada (1980) and could be ascribed to the ascending and descending movements of the upwelled water at, respectively, the northern and southern parts of the "Banc d'Arguin" (Mittlstaedt, 1974). Over the shelf, within the "Banc d'Arguin", the values of primary production given by the two model computations differ by a factor of 2 because of a lower photosynthetic efficiency and lower visibility assigned to this area when the provinces were differentiated.

In open ocean waters, the choice of homogenous or heterogeneous case on computing the daily rate of phytoplankton photosynthesis does not significantly affect the final values in the region south of 21°N (Fig. 7). North of 21°N , however, primary production decreases substantially when accounting for differences in the parameters among provinces. The calculated mean value of production, $\sim 0.5 \text{ gC}\cdot\text{m}^{-2}\cdot\text{d}^{-1}$, corresponding to the "blue waters" shown by the CZCS chlorophyll map, is similar to other computed values for open ocean (Platt *et al.*, 1991) and to *in situ* measurements in central oceanic gyres (Marra and Heinemann, 1987).

Although the model seems to give reasonable results, the power of a comparative study of local primary production values is limited by the variability over time and space of the biological processes which, in this area of study, depend strongly on the hydrodynamics. On the other hand, the efficiency of the model can be assessed by comparing averaged primary production values over large areas, *e.g.*, the northern and southern parts of the studied area on either side of 21°N of latitude. Bricaud *et al.* (1987) have computed the daily rate of primary production over the same area as that described in this work, and using CZCS chlorophyll data which included the same scene applied here. The model of Bricaud *et al.* (1987) corresponds, however, to a site-specific model based on an empirical relationship between production (normalized to PAR) and surface (or integrated) pigment concentration. Although this type of model is of limited use, it does provide precise results for the region and time period over which the empirical relationship has been adapted. Conversely, the analytical (or semi-analytical) model used in this work has a more general applicability since the carbon uptake rate by phytoplankton is formulated from first principles of photosynthetic physiology. For this reason, however, such a model may become less efficient in determining the production rate at a regional scale when compared with a strictly empirical formulation only valid for that region. Table 2 summarizes the water column integrated daily rate

of photosynthesis in the area of study obtained by Bricaud *et al.* (1987) and by the present computations. In both regions, north and south of 21°N, the mean values obtained in this work are close to those of Bricaud *et al.* (1987), as well as those reported by Dugdale *et al.* (1989) using a "satellite" model of new production in upwelling regions based on the adaptation rate of nitrate uptake by phytoplankton. Systematically lower estimates from the analytical model are only due to the fact that computations were extended from the coastline to 21°W of longitude instead of 20°W as in Bricaud *et al.* (1987), giving more weight to lower open ocean production in the averaging process. For the same area but extended to 24°W, Bricaud *et al.* (1987) computed integrated production values of 0.44 gC.m⁻².d⁻¹ and 0.76 gC.m⁻².d⁻¹ for the regions north and south of 21°N, respectively.

CONCLUSION

This work clearly shows that the application of analytical or semi-analytical models to determine the oceanic primary production from satellite data can be extended to highly dynamic environment such as an upwelling centre where, so far, only site-specific formulation could give reasonable results. At present, however, the scarcity of photosynthesis *versus* light measurements may limit the accuracy of these

models, since one has to accommodate several necessary assumptions to select the appropriate parameters.

The assumption of homogeneity in the bio-optical parameters of seawater and the atmospheric conditions provides a good approximation to the absolute values of the daily rate of primary production when averaged over the entire studied area which includes various oceanic regimes. The spatial distribution of these values, however, remains dependent on the chlorophyll concentration, leading to values which are too high near the coast and in open ocean waters. On the other hand, phytoplankton productivity is probably underestimated at the shelf-break, where upwelling activity is at a maximum. Thus, the differentiation of bio-geochemical provinces and the specification of the parameters relevant to each of them are important steps in studying the mean and variations of primary production in marine waters.

Acknowledgments

We thank Drs. A. Morel, J. Neveux, and D. Antoine for sending us their detailed data and allowing us to use them in this work. We are also indebted to Drs. T. Platt and S. Sathyendranath for providing a copy of their computation codes to determine primary production from satellite. Finally, the manuscript benefited from the comments and suggestions of Dr. O. Ulloa and an anonymous reviewer.

REFERENCES

- Abbott M.R. and D.B. Chelton (1991). Advances in passive remote sensing of the ocean. *Reviews of Geophysics*, Suppl. U.S. Nat. Report, 571-589.
- André J.M. and A. Morel (1991). Atmospheric corrections and interpretation of marine radiances in CZCS imagery: revisited. *Oceanologica Acta*, **14**, 3-22.
- Balch W., R. Evans, J. Brown, G. Feldman, C. McClain and W. Esaias (1992). The remote sensing of ocean primary productivity: use of a new data compilation to test satellite algorithms. *J. Geophys. Res.*, **97**, 2279-2293.
- Barale V. and P. Schlittenhardt (1993). *Ocean colour: theory and applications in a decade of CZCS experience*. Kluwer Acad. Pub., 367 p.
- Bird R.E. (1984). A simple, solar spectral model for direct-normal and diffuse horizontal irradiance. *Solar Energy*, **32**, 461-471.
- Bird R.E. and C. Riordan (1986). Simple solar spectral model for direct and diffuse irradiance on horizontal and tilted planes at the earth's surface for cloudless atmospheres. *J. Climate Appl. Meteorol.*, **25**, 87-97.
- Bricaud A. and A. Morel (1987). Atmospheric corrections and interpretation of marine radiances in CZCS imagery: use of a reflectance model. *Oceanologica Acta*, SP, 33-49.
- Bricaud A., A. Morel and J.M. André (1987). Spatial / temporal variability of algal biomass and potential productivity in the Mauritanian upwelling zone, as estimated from CZCS data. *Adv. Space Res.*, **7**, 53-62.
- Bricaud A., A. Morel and L. Prieur (1983). Optical efficiency factors of some phytoplankters. *Limnol. Oceanogr.*, **28**, 816-832.
- Dugdale R.C., A. Morel, A. Bricaud and F.P. Wilkerson (1989). Modeling new production in upwelling centers: a case study of modeling new production from remotely sensed temperature and color. *J. Geophys. Res.*, **94**, 18,119 - 18,132.
- Campbell J.W. and J.E. O'Reilly (1988). Role of satellites in estimating primary productivity on the northwest Atlantic continental shelf. *Continental Shelf Res.*, **8**, 179-204.
- Eppley R.W., E. Steward, M.R. Abbott and U. Heyman (1985). Estimating ocean primary production from satellite chlorophyll: Introduction to regional difference and statistics for the Southern California Bight. *J. Plankt. Res.*, **7**, 57-70.
- Estrada M. (1980). Phytoplankton biomass and production in the upwelling region of NW Africa. Relationships with hydrographic parameters. *Mar. Biol.*, **60**, 63-71.
- Gordon H.R., J.W. Brown and R.H. Evans (1988). Exact Rayleigh scattering calculations for use with the Nimbus-7 Coastal Zone Color Scanner. *Appl. Opt.*, **27**, 862-871.
- Gordon H.R. and D.K. Clark (1980). Remote sensing of optical properties of a stratified ocean: an improved interpretation. *Appl. Opt.*, **19**, 3428.
- Gregg W.W. and K.L. Carder (1990). A simple spectral solar irradiance model for cloudless maritime atmospheres. *Limnol. Oceanogr.*, **35**, 1657-1675.

- Hagen E. and R. Schemainda (1987). On the zonal distribution of south Atlantic central water (SACW) along a section off Cape Blanc, Northwest Africa. *Oceanologica Acta*, SP, 61-70.
- Hempel G. (1982). The Canary Current: studies of an upwelling system. *Rapp. P.-v. Réun. Cons. int. Explor. Mer.*, **180**, 455 p.
- Huntsman S.A. and R.T. Barber (1977). Primary production off northwest Africa: the relationship to wind and nutrient conditions. *Deep Sea Res.*, **24**, 25-33.
- Iqbal M. (1983). *An introduction to solar radiation*. Academic Press, 390 p.
- Kywalyanga M., T. Platt and S. Sathyendranath (1992). Ocean primary production calculated by spectral and broad-band models. *Mar. Ecol. Prog. Ser.*, **85**, 171-185.
- Lloyd I.J. (1971). Primary production off the coast of northwest Africa. *Rapp. P.-v. Réun. Cons. int. Explor. Mer.*, **33**, 312-323.
- Manriquez M. and F. Fraga (1978). Hidrografía de la región de afloramiento del noroeste de Africa: campaña "Atlor VII". *Res. Exp. Cient. B/o Cornide de Saavedra*, **7**, 1-32.
- Marra J. and K.R. Heinemann (1987). Primary production in the North Pacific Central Gyre: some new measurements based on ¹⁴C. *Deep-Sea Res.*, **34**, 1821-1829.
- Minas H.J., L.A. Codispoti and R.C. Dugdale (1982). Nutrients and primary production in the upwelling region off northwest Africa. *Rapp. P.-v. Réun. Cons. int. Explor. Mer.*, **180**, 148-183.
- Mittlestaedt E. (1974). Some aspects of the circulation in the Northwest African upwelling area off Cape Blanc. *Téthys*, **6**, 89-92.
- Mittlestaedt E. (1991). The ocean boundary along the northwest African coast: circulation and oceanographic properties at the sea surface. *Prog. Oceanogr.*, **26**, 307-355.
- Morel A. (1974). Optical properties of pure water and pure sea water. In: *Optical aspects of oceanography*, N.G. Jerlov and E. Steeman-Nielsen, editors. Academic Press, 1-24.
- Morel A. (1980). In-water and remote measurement of ocean colour. *Boundary Layer Meteorol.*, **18**, 177-201.
- Morel A. (1988). Optical modeling of the upper ocean in relation to its biogenous matter content (csea 1 waters). *J. Geophys. Res.*, **93**, 10,749-10,768.
- Morel A. (1991). Light and marine photosynthesis: a spectral model with geochemical and climatological implications. *Prog. Oceanogr.*, **26**, 263-306.
- Morel A. and J.M. André (1991). Pigment distribution and primary production in the western Mediterranean as derived and modeled from Coastal Zone Color Scanner observations. *J. Geophys. Res.*, **96**, 12,685-12,698.
- Morel A. and L. Prieur (1976). Irradiation journalière en surface et mesures des éclaircissements sous-marins; flux de photons et analyse spectrale. In: *Résultats de la campagne CINECA 5 -J. Charcot Capricorne*. Publication CNEXO, 10 (section 1.1.10), 1-257.
- P.F.O. (Programme Flux Océaniques) Report (1989). Opération EUMELI, flux de matière dans l'Atlantique tropical en régime eutrophe, mésotrophe et oligotrophe. Rapport n° 2 (2^e édition), 39 p.
- Platt T., C.M. Caverhill and S. Sathyendranath (1991). Basin-scale estimates of oceanic primary production by remote sensing: the North Atlantic. *J. Geophys. Res.*, **96**, 15,147-15,159.
- Platt T. and S. Sathyendranath (1988). Oceanic primary production: estimation by remote sensing at local and regional scales. *Science*, **241**, 1613-1620.
- Platt T. and S. Sathyendranath (1991). Biological production models as elements of coupled, atmosphere-ocean models for climate research. *J. Geophys. Res.*, **96**, 2585-2592.
- Platt T. and S. Sathyendranath (1993). Estimators of primary production for interpretation of remotely-sensed data on ocean colour. *J. Geophys. Res.*, **98**, C 8., 14, 561-14, 576.
- Platt T., S. Sathyendranath, C.M. Caverhill and M.R. Lewis (1988). Ocean primary production and available light: further algorithms for remote sensing. *Deep-Sea Res.*, **35**, 855-879.
- Platt T., S. Sathyendranath, O. Ulloa, W.G. Harrison, N. Hoepffner and J. Goes. (1992). Nutrient control of phytoplankton photosynthesis in the western North Atlantic. *Nature*, **356**, 229-231.
- Prieur L. and S. Sathyendranath (1981). An optical classification of coastal and oceanic waters based on the specific spectral absorption curves of phytoplankton pigments, dissolved organic matter and other particulate materials. *Limnol. Oceanogr.*, **26**, 671-689.
- Richards F.A. (1981). Coastal Upwelling. Coastal and Estuarine Sciences 1, American Geophysical Union, 529 p.
- Sathyendranath S. and T. Platt (1988). The spectral irradiance field at the surface and the interior of the ocean: a model for application in oceanography and remote sensing. *J. Geophys. Res.*, **93**, 9270-9280.
- Sathyendranath S. and T. Platt (1989). Remote sensing of ocean chlorophyll: consequence of non-uniform pigment profile. *Appl. Opt.*, **28**, 490-495.
- Sathyendranath S. and T. Platt (1991). Angular distribution of the submarine light field: modification by multiple scattering. *Proc. R. Soc. Lond. A*, **433**, 287-297.
- Sathyendranath S., T. Platt, C.M. Caverhill, R.E. Warnock and M.R. Lewis (1989). Remote sensing of oceanic primary production: computations using a spectral model. *Deep-Sea Res.*, **36**, 431-453.
- Sathyendranath S., T. Platt, E.P.W. Horne, W.G. Harrison, O. Ulloa, R. Outerbridge and N. Hoepffner (1991). Estimation of new production in the ocean by compound remote sensing. *Nature*, **353**, 129-133.
- Schulz S. (1982). A comparison of primary production in upwelling regions off northwest and southwest Africa. *Rapp. P.-v. Réun. Cons. int. Explor. Mer.*, **180**, 202-204.
- Sturm B. (1986). Correction of the sensor degradation of the Coastal Zone Color Scanner on Nimbus-7. ESA-EARSel proceedings, Lyngby, Denmark (June 1986), ESA-SP, 258.
- Sturm B. (1993). CZCS data processing algorithms. In: Ocean colour: theory and applications in a decade of CZCS experience, V. Barale and P. Schlittenhardt, editors Kluwer Acad. Pub., 95-117.
- Van Heuklon T.K. (1979). Estimating atmospheric ozone for solar radiation models. *Solar Energy*, **22**, 63-68.